An algorithm for the three-dimensional inversion of magnetotelluric data

Colin G. Farquharson, Douglas W. Oldenburg, UBC–Geophysical Inversion Facility, U. of British Columbia, Vancouver, Canada, Eldad Haber, EMI–Schlumberger, Richmond, CA, Roman Shekhtman, UBC–GIF.*

Summary

We present an algorithm for inverting magnetotelluric data to recover a three-dimensional conductivity model of the Earth. The algorithm is an iterative, linearised, minimum-structure procedure within which the solution of the forward problem, the application of the Jacobian matrix of sensitivities, and the solution of the matrix equation are all done using sparse matrix-vector operations. Consequently, the algorithm is extremely efficient in its use of memory, making three-dimensional inversions feasible.

Introduction

The magnetotelluric (MT) technique, which uses the natural variations of the Earth's magnetic field as its source, is sensitive to the Earth's conductivity structure to greater depths than any electromagnetic technique using man-made sources. Its classic application is to the study of the crust and upper mantle. However, the MT method also plays a significant role in hydrocarbon exploration when geology is sufficiently complex or of a certain type that traditional seismic methods fail, and is playing an ever more important role in mineral exploration as interest in discovering deeper targets increases.

The improvements in speed and memory of computers has now made the three-dimensional inversion of geophysical electromagnetic data conceivable, and there have been a number of recent reports of the development of inversion algorithms for MT data, for example, Newman and Alumbaugh (2000), Hursán and Zhdanov (2001), Uchida et al. (2001), Mackie et al. (2001).

Here we present a further algorithm for the three-dimensional inversion of MT data. Its overall framework is that of a typical iterative, linearised, minimum-structure inversion procedure, and as such is similar to other algorithms. However, it differs in many of the details. It is built upon a forward-modelling procedure that decomposes the electric field into vector and scalar potentials to avoid problems with the null space of the curl operator, efficiently solves the matrix equation using a preconditioned Krylov space method, and can cope with large conductivity contrasts. The matrix equation at each iteration of the inversion algorithm is solved using a similar Krylov space method, which requires only matrix-vector products, not the explicit generation and storage of the inverse of the matrix. As such, only the product of the Jacobian matrix (or its transpose) with a vector is ever needed, and this can be done efficiently using the forward-modelling solution procedure with a modified right-hand side. Hence, the whole inversion algorithm involves only sequences of sparse matrix-vector products, making it very effective for large-scale problems.

Forward modelling

Our forward-modelling procedure is based on that of Haber et al. (2000a). Those authors concentrated on controlled sources. Here we summarise the modifications required for the MT problem, with only brief mention of the points common to both procedures.

Haber et al. (2000a) decompose the electric field into vector and scalar potentials:

$$\mathbf{E} = \mathbf{A} + \nabla\phi, \tag{1}$$

and impose the Coloumb gauge condition:

$$\nabla \cdot \mathbf{A} = 0 \tag{2}$$

to render the decomposition unique. (See also Everett and Schultz, 1996; LaBrecque, 1999.) This decomposition explicitly splits the electric field into a part ($\mathbf{A}$) residing in the active space of the curl operator, and a part ($\nabla\phi$) residing in its null space. Eliminating the H-field from Maxwell's two curl equations, and introducing eqs. (1) & (2) gives

$$\nabla^2\mathbf{A} + i\omega\mu_0\sigma(\mathbf{A} + \nabla\phi) = 0, \tag{3}$$

where ω is the angular frequency, μ_0 is the magnetic permeability of free space, $\sigma = \sigma(\mathbf{r})$ is the electrical conductivity of our Earth model, $i = \sqrt{-1}$, and the quasi-static assumption and a time-dependence of $e^{-i\omega t}$ have been assumed. For the purposes of the discussion here, we consider the above equation to be a homogeneous equation: how the "source" of the MT fields is implemented is dealt with below. The definition of current density, and the statement that it is divergence free (again ignoring any sources) are

$$\mathbf{J} = \sigma(\mathbf{A} + \nabla\phi), \tag{4}$$

and

$$\nabla \cdot \mathbf{J} = 0. \tag{5}$$

For both the forward and inverse problems, we discretise our Earth model into a rectangular grid of cells with the conductivity considered to be uniform within each cell. To obtain a numerical solution, the scalar potential is approximated by its values at the cell centres, and the vector potential and current density by their normal components at the centres of the cell faces. A system of equations is obtained by applying a finite volume technique to

eqs. (3)–(5) (see Haber et al. 2000a). This involves the harmonic averaging of the conductivities in neighbouring cells. Once this has been done, the components of the current density can be eliminated from the algebraic equations, giving

$$\begin{pmatrix} L + i\omega\mu_0 S & i\omega\mu_0 S G \\ D S & D S G \end{pmatrix} \begin{pmatrix} A \\ \phi \end{pmatrix} = 0, \tag{6}$$

where A now represents the vector containing the values of the components of the vector potential on the mesh, and ϕ represents the vector of values of the scalar potential. In addition, L represents the typical discretisation of the Laplacian operator, S represents the averaged cell conductivities, and G and D are the discretisations of the gradient and divergence operators. The matrix in eq. (6) is extremely sparse.

We consider two different solution methods for the MT forward-modelling problem. The first involves expressing the electric field as the sum of a primary part associated with a background model and a secondary part arising from the difference between the actual model and the background. Equation (6) then becomes

$$\begin{pmatrix} L + i\omega\mu_0 S & i\omega\mu_0 S G \\ D S & D S G \end{pmatrix} \begin{pmatrix} A^s \\ \phi^s \end{pmatrix} = \begin{pmatrix} -i\,\omega\mu_0 \Delta S E_p \\ -D \Delta S E_p \end{pmatrix}, \tag{7}$$

where $\Delta S = S - S_p$ is the difference between the averaged conductivities of the actual model and those of the background, E_p is the primary electric field, and A^s & ϕ^s are the secondary potentials. The background model can be anything, although we have only considered horizontally-layered models. The boundary conditions for this solution method are that the tangential component of $\nabla \times \mathbf{A}^s$, the normal component of $\mathbf{A}^s$, and the normal derivative of ϕ^s all vanish on the mesh boundaries.

The second method of solution for the MT problem involves solving eq. (6) directly for the total field. In this case, the tangential component of $\nabla \times \mathbf{A}$ (that is, the H-field) and the normal component of $\mathbf{J}$ are specified on the boundaries. These values are computed for the one- or two-dimensional conductivity model that is appropriate for each boundary.

The matrix equations in both of the above methods are solved using a stabalised bi-conjugate gradient algorithm. This requires only the products of the sparse matrix in eqs. (6) & (7) with a vector. An incomplete LU decomposition of the L and $D\,S\,G$ blocks is used as a preconditioner.

To finish the forward-modelling process for the MT problem, the horizontal components of the E- & H-fields are computed for two different polarisations of the source field: one for an x-directed H-field at the top of the mesh, and the other for a y-directed H-field. The components, Z_{xx}, Z_{xy}, Z_{yx} & Z_{yy}, of the impedance tensor are then computed from the solution of:

$$\begin{pmatrix} E_x^x & E_x^y \\ E_y^x & E_y^y \end{pmatrix} = \begin{pmatrix} Z_{xx} & Z_{xy} \\ Z_{yx} & Z_{yy} \end{pmatrix} \begin{pmatrix} H_x^x & H_x^y \\ H_y^x & H_y^y \end{pmatrix}, \tag{8}$$

where the superscripts indicate the source field polarisation.

Inversion

The main features of our inversion algorithm – the minimisation of a combination of data-misfit and model complexity, and solution by means of an iterative Gauss-Newton procedure based on the linearised approximation of the relationship between the model parameters and observations – are standard. However, because the three-dimensional inversion of electromagnetic data is so computationally intensive, it is critical that the components of the algorithm are efficiently implemented. The algorithm used here is the Gauss-Newton algorithm of Haber et al. (2000b), with the necessary modifications for inverting MT data.

Our solution to the inverse problem is via the minimisation of the objective function:

$$\Phi = \phi_d + \beta\,\phi_m, \tag{9}$$

where ϕ_d is a measure of data-misfit, ϕ_m is a measure of the amount of structure in the Earth model, and β is the trade-off or regularisation parameter that balances the effects of the two terms. The measure of misfit we use here is the traditional sum-of-squares misfit:

$$\phi_d = \left\| \mathbf{W}_d \left(\mathbf{d}^{\text{obs}} - \mathbf{d}^{\text{prd}} \right) \right\|^2, \tag{10}$$

where $\mathbf{d}^{\text{obs}}$ is the vector of observations, $\mathbf{W}_d$ is a diagonal matrix whose elements at the reciprocals of the measurement uncertainties, and $\|\cdot\|$ represents the l_2-norm. The data, $\mathbf{d}^{\text{prd}}$, produced by the forward-modelling for a particular Earth model can be represented by:

$$\mathbf{d}^{\text{prd}} = Q(\mathbf{u}_x, \mathbf{u}_y), \tag{11}$$

where $\mathbf{u}_x$ & $\mathbf{u}_y$ are the solutions of eq. (7) (or eq. 6) for the two polarisations of the source field. The operator Q incorporates both the calculation of the horizontal components of the E- & H-fields at each observation location from the values of the vector and scalar potentials on the mesh, and the calculation of the impedances (see eq. 8). The former operation is the same as that of the Q matrix of Haber et al. (2000b).

The measure of model structure is the typical

$$\phi_m = \sum_{k=1}^{4} \alpha_k \left\| \mathbf{W}_k \left(\mathbf{m} - \mathbf{m}^{\text{ref}} \right) \right\|^2, \tag{12}$$

where $\mathbf{W}_1$ is a diagonal matrix and $\mathbf{W}_2$, $\mathbf{W}_3$ & $\mathbf{W}_4$ are the first order finite-difference matrices in the x-, y- & z-directions for the mesh, and $\mathbf{m}^{\text{ref}}$ is a reference model. The vector $\mathbf{m}$ contains the parameters describing the model: the logarithms of the cell conductivities.

At the $(n+1)$th iteration in the minimisation of the objective function, the Gauss-Newton method requires the

solution of:

$$\left(\mathbf{J}^T\mathbf{W}_d^T\mathbf{W}_d\mathbf{J} + \beta\,\mathbf{W}^T\mathbf{W}\right)\delta\mathbf{m} = -\mathbf{J}^T\mathbf{W}_d^T\mathbf{W}_d\left(\mathbf{d}^{\rm obs} - \mathbf{d}^n\right) - \beta\mathbf{W}^T\mathbf{W}\left(\mathbf{m}^n - \mathbf{m}^{\rm ref}\right), \quad (13)$$

where $\mathbf{m}^n$ is the vector of model parameters from the preceding iteration, $\mathbf{J} = \mathbf{J}(\mathbf{m}^n)$ is the Jacobian matrix of sensitivities, $\mathbf{W}$ is such that $\mathbf{W}^T\mathbf{W} = \sum \alpha_k \mathbf{W}_k^T\mathbf{W}_k$, and $\delta\mathbf{m}$ is the perturbation to be added to $\mathbf{m}^n$ to give the new model.

Following Haber et al. (2000b), we solve eq. (13) using an inexact preconditioned conjugate gradient algorithm. The preconditioner is the incomplete LU decomposition of the matrix $\left(\mathbf{W}^T\mathbf{W} + 0.1\,\mathbf{I}\right)$, where $\mathbf{I}$ is the identity matrix. This method of solution requires only the operation of $\mathbf{W}^T\mathbf{W}$, $\mathbf{J}$ and $\mathbf{J}^T$ on a vector. These multiplications (described below for the Jacobian) can be done entirely with sparse matrix-vector operations.

At present, our inversion algorithm uses the primary-secondary method of solution for the forward modelling (see eq. 7). Differentiating eq. (7) with respect to the model parameters, using the chain rule, and rearranging, gives

$$\tilde{\mathbf{A}}\,\frac{\partial\mathbf{u}^s}{\partial\mathbf{m}} = \frac{\partial\mathbf{b}}{\partial\mathbf{m}} - \frac{\partial(\tilde{\mathbf{A}}\mathbf{u}^s)}{\partial\mathbf{m}}, \quad (14)$$

where $\tilde{\mathbf{A}}$, $\mathbf{u}^s$, and $\mathbf{b}$ are the matrix, solution vector and right-hand side of eq. (7). Expressions for the matrices on the right-hand side of eq. (14) follow directly from the differentiation of the elements of $\tilde{\mathbf{A}}$.

Consider now the Jacobian matrix of sensitivities:

$$\mathbf{J} \equiv \frac{\partial\mathbf{d}^{\rm prd}}{\partial\mathbf{m}} = \frac{\partial}{\partial\mathbf{m}}Q(\mathbf{u}_x, \mathbf{u}_y), \quad (15)$$

$$= \frac{\partial Q}{\partial\mathbf{u}_x^s}\,\frac{\partial\mathbf{u}_x^s}{\partial\mathbf{m}} + \frac{\partial Q}{\partial\mathbf{u}_y^s}\,\frac{\partial\mathbf{u}_y^s}{\partial\mathbf{m}}. \quad (16)$$

The matrix $\partial Q/\partial\mathbf{u}^s$ is straightforward to determine given the expressions for the elements of the impedance tensor in terms of the horizontal E- & H-fields. Hence, the procedure for computing the action of the Jacobian matrix on a vector is as follows (see also Mackie and Madden, 1993; Mackie et al., 2001). The vector is first pre-multiplied by the right-hand side of eq. (14) with $\mathbf{b}$ and $\mathbf{u}^s$ for the first source polarisation. Equation (14) is then solved with this new right-hand side. This is done using the same procedure as for the forward modelling. The solution is then pre-multiplied by $\partial Q/\partial\mathbf{u}_x^s$. The second term in eq. (16) is obtained in the same way, but using $\mathbf{b}$ and $\mathbf{u}^s$ for the second polarisation. The action of the transpose of the Jacobian matrix on a vector is accomplished in an analogous manner.

Once $\delta\mathbf{m}$ has been found at a particular iteration, the new model is given by $\mathbf{m}^{n+1} = \mathbf{m}^n + \gamma\,\delta\mathbf{m}$, where γ $(0 < \gamma \leq 1)$ is determined by a line search such that the objective function is decreased. In the present version of the algorithm, the trade-off parameter β is prescribed by a cooling schedule.

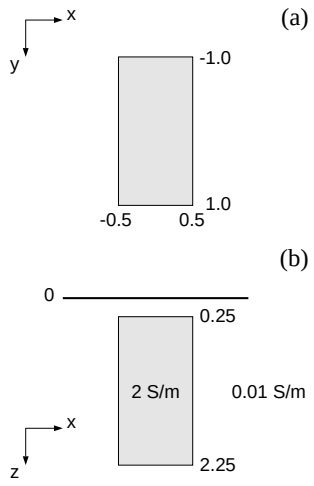

Fig. 1: The COMMEMI 3D-1 model of Zhdanov et al (1997) which was used for the synthetic example in this abstract. Panel (a) shows a plan view and panel (b) shows a vertical section through the conductive block. The distances are in kilometres.

Example

We briefly illustrate the abilities of our inversion algorithm with its performance on a simple synthetic data-set. The real and imaginary parts of all four elements of the impedance tensor were computed for three frequencies (0.1, 1 & 10 Hz) at 81 locations over the COMMEMI 3D-1 model (Zhdanov et al. 1997; see Fig. 1). The mesh contained 37, 41 & 24 cells in the x-, y- & z-directions, respectively. Random noise was added to the computed impedances to give the data-set that was inverted. The standard deviation of the noise was 5 % of the magnitude of a datum, or one-half of the average magnitude of all the off-diagonal elements of the impedance tensor, whichever was larger. The off-diagonal impedances for 10 Hz are plotted in Fig. 2.

The inversion took a dozen iterations to reduce the misfit to 2100. (There were 1296 data.) The forward-modelled data for the final model are shown in Fig. 3. The final model was the typical smeared-out image of the true model. Both the starting and reference models were homogeneous halfspaces of 0.01 S/m. The trade-off parameter was specified to decrease exponentially from 1000 to 1. The dozen iterations required 24 hours running on three 1 GHz Pentium III computers.

Acknowledgments

This work was funded by NSERC and the "IMAGE" Consortium, of which the following are members: AGIP, Anglo American, Billiton, Cominco, Falconbridge, INCO,

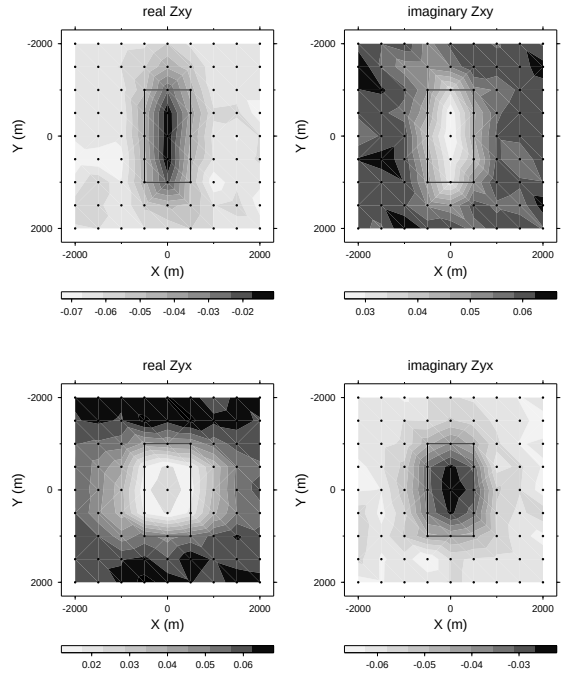

Fig. 2: The real and imaginary parts of the off-diagonal tensor elements at 10 Hz from the data-set that was inverted in the example. The 81 observation locations are shown by the dots. The rectangles indicate the outline of the conductive block.

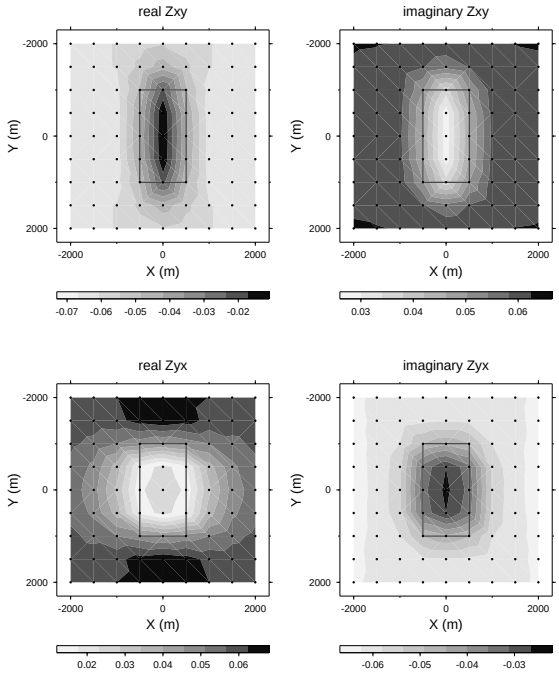

Fig. 3: The forward-modelled off-diagonal tensor elements at 10 Hz for the final model in the example inversion.

MIM, Muskox Minerals Newmont, Placer Dome, and Rio Tinto. We are grateful for their participation.

References

Everett, M. E., and Schultz, A., 1996, Geomagnetic induction in a heterogeneous sphere: Azimuthally symmetric test computations and the response of an undulating 660-km discontinuity: J. Geophys. Res., 101, 2765–2783.

Haber, E., Ascher, U. M., Aruliah, D. A., and Oldenburg, D. W., 2000a, Fast Simulation of 3D electromagnetic problems using potentials: J. Comp. Phys., 163, 150–171.

Haber, E., Ascher, U. M., and Oldenburg, D. W., 2000b, On optimization techniques for solving nonlinear inverse problems: Inverse Problems, 16, 1263–1280.

Hursán, G., and Zhdanov, M. S., 2001, Rapid 3-D magnetotelluric and CSAMT inversion: 71st Ann. Internat. Mtg., Soc. Expl. Geophys., 1493–1496.

LaBrecque, D. J., 1999, Finite-difference modeling of 3-D EM fields with scalar and vector potentials: in Three-Dimensional Electromagnetics, Oristaglio, M., and Spies, B., eds., Soc. Expl. Geophys., 146–160.

Mackie, R. L., and Madden, T. R., 1993, Three-dimensional magnetotelluric inversion using conjugate gradients: Geophys. J. Int., 115, 215–229.

Mackie, R. L., Rodi, W., and Watts, M. D., 2001, 3-D magnetotelluric inversion for resource exploration: 71st Ann. Internat. Mtg., Soc. Expl. Geophys., 1501–1504.

Newman, G. A., and Alumbaugh, D. L., 2000, Three-dimensional magnetotelluric inversion using non-linear conjugate gradients: Geophys. J. Int., 410, 140–424.

Uchida, T., Lee, T. J., Sasaki, Y., Honda, M., Andan, A., and Andan, A., 2001, Three-dimensional inversion of magnetotelluric data at the Bajawa geothermal field, eastern Indonesia: 71st Ann. Internat. Mtg., Soc. Expl. Geophys., 1497–1500.

Zhdanov, M. S., Varentsov, I. M., Weaver, J. T., Golubev, N. G., and Krylov, V. A., 1997, Methods for modelling electromagnetic fields: Results from COMMEMI – the international project on the comparison of modelling methods for electromagnetic induction: J. Appl. Geophys., 37, 133–271.